Revista Cubana de Ingeniería Vol.XIV (2) e359 (2023) ISSN: 2223-1781

**Artículo Original**

# 3D-Printed Myoelectric Arm Prosthesis Prototype for Children with Upper Limb Agenesis: A Feasibility Study

# Prototipo de Prótesis de Brazo Mioeléctrica Impresa en 3D para Niños con Agenesia de Miembro Superior: Un Estudio de Viabilidad

**Augusto Perez[1], Milky Rodriguez[1], Clarissa Nieto[2], Graciela Ambulo[2], Mario Pitti[1], Librada Villareal[1], Hector Mendoza[1], Denia Rodriguez[3], Ericka Matus[1], Ernesto Ibarra[4], Jay Molino[1,5]**

[1]Faculty of Biosciences and Public Health, Universidad Especializada de las Américas (UDELAS), Corregimiento de Ancón, Panama City, Republic of Panama.
[2]Instituto de Salud Física y Deportiva, Universidad Especializada de las Américas (UDELAS), Corregimiento de Ancón, Panama City, Republic of Panama.
[3]Faculty of Information Technology, Electronics, and Communication, Universidad de Panama, Octavio Mendez Pereira Campus, 3366, Panama, Panama.
[4]Faculty of Electrical Engineering, Universidad Tecnológica de Panamá, Campus Victor Levi Sasso, Panama, Panama.
[5]Sistema Nacional de Investigación (SNI), SENACYT, Panamá.

* Autor de correspondencia: jay.molino@udelas.ac.pa

## Resumen

Las amputaciones congénitas de miembro superior son una condición médica que afecta a millones de personas en todo el mundo. Las causas pueden ser el resultado de factores genéticos, problemas durante el desarrollo fetal, alteraciones cromosómicas o factores ambientales, y van desde la ausencia parcial de un dedo hasta la ausencia completa de una extremidad.
Una de las causas más comunes es la agenesia de miembro superior, que puede ser parcial o completa. Condiciones como la acondroplasia, la ausencia radial, la hemimelia fibular o la amelia pueden provocar la ausencia o el subdesarrollo de extremidades. Aunque existen tratamientos como las prótesis para miembro superior que mejoran la calidad de vida de las personas amputadas, pueden ser costosas y difíciles de obtener.
En este estudio, se desarrolló un prototipo de prótesis de brazo de bajo costo para pacientes pediátricos con agenesia de miembro superior. El prototipo se diseñó y fabricó utilizando métodos de manufactura digital aditiva, específicamente la impresión 3D. Las partes mecánicas se fabricaron con la impresora Creality Ender-5 Plus, mientras que los componentes electrónicos se diseñaron e implementaron utilizando un Arduino Uno.
Con un peso de 250 gramos y un costo de fabricación de aproximadamente US$500, el prototipo puede realizar un agarre cilíndrico con una fuerza de sujeción de hasta 10 newtons. Los resultados del análisis de elementos finitos muestran que el prototipo tiene un margen de seguridad suficiente para soportar cargas de hasta 2 N. Además, el desplazamiento máximo registrado de 0,45 mm se considera aceptable.
Los resultados de este estudio demuestran que el prototipo de prótesis para antebrazo es una solución viable para pacientes pediátricos con agenesia de miembro superior. El prototipo es funcional, seguro y tiene un costo relativamente bajo.

**Palabras claves:** agenesia, bajo costo, impresión 3D, prótesis de miembro superior.

## Abstract

Congenital upper limb amputations are a medical condition affecting millions of people worldwide. Causes can stem from genetic factors, issues during fetal development, chromosomal abnormalities, or environmental factors, ranging in severity from partial finger absence to complete limb absence. One of the most common causes is upper limb agenesis, which can be partial or complete. Conditions like achondroplasia, radial absence, fibular hemimelia, or amelia may result in limb absence or underdevelopment. While treatments such as upper limb prosthetics exist to enhance the quality of life for amputees, they can be costly and challenging to acquire.

This study developed a low-cost arm prosthesis prototype for pediatric patients with upper limb agenesis. The prototype was designed and manufactured using additive digital manufacturing methods, specifically 3D printing. Mechanical parts were produced with the Creality Ender-5 Plus printer, while electronic components were designed and implemented using an Arduino Uno.

Weighing 250 grams with a manufacturing cost of approximately US$500, the prototype can perform a cylindrical grip with a gripping force of up to 10 newtons. Finite element analysis results demonstrate that the prototype has sufficient safety margins to withstand loads of up to 2 N. Additionally, the recorded maximum displacement of 0.45 mm is deemed acceptable.

The study's outcomes reveal that the forearm prosthesis prototype is a viable solution for pediatric patients with upper limb agenesis. The prototype is functional, safe, and relatively low-cost.

**Keywords:** Agenesia, low cost, 3D printing, upper limb prosthesis.

## 1. Introduction

Upper limb amputations and malformations affect a variable proportion of the world population, with estimates ranging from 4 to 5 per 10,000 to 1 per 100 live births (Bethge, Von Groote, Giustini, & Gutenbrunner, 2014). In the case of congenital upper limb malformations, an incidence of around 2.3 per 1,000 live births is estimated (Gishen & Askari, 2014). In France, upper limb transverse agenesis occurs 1.7 cases per 10,000 births, or approximately 150 cases per year (Ayuso, 2018).

In the United States, the prevalence of these conditions ranges from 0.16% to 0.18%, with significant regional and ethnic variations. Research in Finland, Canada, and Australia reports 3.4 to 5.3 per 10,000 live births (Dy, Swarup, & Daluiski, 2014). In Colombia, upper limb malformations are the third most prevalent, with polydactyly being the most common, with an incidence of 21.2 per 10,000 live births (Zarante, Franco, López, & Fernández, 2010).

According to the 2010 census in Panama, 2.9% of the total population has some form of disability, with physical disability being the most prevalent at 30.1%. This category includes people with physical limitations due to accidents, diseases, strokes, amputations, or congenital malformations that affect dexterity in daily activities.

Upper limb prostheses have been significantly developed in response to these needs using technologies such as 3D printing. These prostheses, for the most part, are high-tech models, including myoelectric variants, that seek to provide more accessible and personalized solutions to individuals with amputations or malformations in the upper extremities (FAULHABER, 2017) (Ottobock, 2017) (Össur, 2018) (Peerdeman, Boere, Witteveen, Huis, & Hermie Hermens, 2017) (Kate, Smit, & Breedveld, 2017)

In the field of open source projects, initiatives such as eNable (Enable Community Foundation, 2017) , Limbitless (Limbitless Solutions, 2016) , NotImpossible (Not Impossible., 2016) , Open Bionics (Open Bionics, 2017) , ROMP (Range of Motion Project., 2015) , and the MHK (My

Human Kit, 2017) community stand out. These projects involve volunteers who leverage accessible 3D technologies to produce prostheses, fostering an exchange of knowledge within their communities. The primary purpose of these activities is to bring new technologies and their products, prostheses, to the people who need them (Koprnicky, 2017).

Regardless of the level, upper limb amputations have a significant functional impact on the affected individuals (Koprnicky, 2017) . The absence of the forearm or hand also has a considerable emotional and psychological effect on the individual (Cabrera, 2012). As an orthopedic and trauma surgeon points out, "If a child born without a hand reaches three months of life without this limb, it will fix in its brain a distorted idea of bimanual (concept of equal arm length)." Replacing the missing limb with a cosmetic prosthesis from the earliest stages of life is imperative to avoid this effect. In this way, the child integrates the equality of the length of their limbs into their cerebral cortex.

Generally, hand prostheses are divided into three categories. First, upper limb cosmetic prostheses are designed to look like natural hands. Some of them are developed as a low-cost, functional cosmetic prosthesis that allows objects to be grasped with a novel alloy wire-reinforced structure. Despite their realistic appearance, cosmetic prostheses do not offer the same functionality for object manipulation as more advanced prostheses. Second, body-powered prostheses are activated by movements of the shoulder pronation of the contralateral limb to the amputation. Today, thanks to 3D printing technology, it is feasible to develop scalable and low-cost pediatric prostheses to meet their rapid growth. However, body-powered prostheses can be challenging, uncomfortable, and heavy. Third, myoelectric prostheses are more advanced thanks to sensors, motors, and batteries. (Bastarrechea, Estrada, Zubrzycki, Torres-Argüelles, & Reynoso, 2020)

The Orthopedic Surgery and Traumatology Manual establishes guidelines for the treatment of upper limb agenesis, suggesting "placing an extension prosthesis early, at the first month of age when the child initiates bimanual, and gradually increasing the complexity of the prosthesis as the patient learns to handle it" (Sociedad Española de Cirugía Ortopédica y Traumatología., 2010) . This early and gradual approach aims to facilitate the patient's adaptation to the prosthesis and optimize its functionality over time.

During the preschool stage, it is crucial to replace the aesthetic hand with a prosthesis that facilitates gripping for object manipulation (MEDIPRAX, 2020) , eventually evolving towards using myoelectric prostheses, which are controlled by electrical impulses generated by muscle contractions. The use of prostheses in children under two years old helps improve their overall well-being and physical health (Sato, Kaji, & Oizumi, 1999), contributes to the formation of a body image with the prosthesis (Sorbye, 1980), and leads to prolonged use of the hand prosthesis (Huizing, Reinders-Messelink, Maathuis, Hadders-Algra, & Sluis, 2010).

The rejection rate of upper limb prostheses in children ranges from 30% to 50%, even higher in cases of reductions below the wrist (Davids, Wagner, & Meyer, 2005). Major reasons for rejection identified by children include (1) limited functionality, (2) discomfort, (3) excessive weight, and (4) unattractive appearance (Vasluian, y otros, 2013) . According to (James, y otros, 2006) , many children with congenital limb deficiency find it easier to perform tasks without prostheses (Budinski, Manojlović, & Knežević, 2021) (Fleming, Huang, Buxton, Hodges, & Huang, 2021)

Family financial resources play a crucial role in prosthesis management, as currently accessible options, such as cable and manual control, have cost around $6,000, excluding electronic mechanisms. Electric motor prostheses range from $4,000 to $8,000, while myoelectric ones can vary from $25,000 to $50,000 (Resnik, y otros, 2012). More advanced and comfortable myoelectric prosthesis alternatives are available for $20,000 to $26,000 (IMPACTO POSITIVO, 2020). These

substantial one-time costs increase due to the frequent need for prosthesis repair and replacement as children grow and experience changes in their physiognomy, leading to a significant increase in lifetime costs associated with limb deficiency (Burn & Gogola, 2016) .. This fact represents an additional burden for families.

Developing a low-cost myoelectric prosthesis through 3D printing capable of performing a cylindrical grip, aims to enable users to acquire the necessary muscle skills for myoelectric prosthesis use in their early development stages, significantly reducing the likelihood of rejection.

Given the limited information in Panama on the prevalence of children with upper limb agenesis amputations and the need for prostheses, a low-cost approach is essential. Considering the country's economic situation, which is affected by unemployment rates and increasing poverty (Banco Mundial, 2021) , justifies the urgency of developing affordable and functionally advanced prostheses.

This study proposes the development of a low-cost arm prosthesis prototype with gripping capability for pediatric patients with upper limb agenesis, considering pediatric patients with transradial amputation aged 1-3 years. These individuals can improve their quality of life by having access to a technologically functional prosthetic limb, aiding in skill development and the execution of daily activities. The main challenge of not using a prosthesis early for patients with agenesis is developing motor skills and forming a balanced perception of bimanually. The lack of a functional prosthesis during the first months and years of life can negatively influence neuromuscular development and body perception.

## 2. Methodology

### *Ethical Considerations*

During the development of this project, special attention has been paid to ethical considerations related to research involving the child population. Comprehensive respect for the participants was ensured by obtaining informed consent from parents or legal guardians before collecting anthropometric data. Additionally, rigorous ethical guidelines were followed when using biometric data, ensuring the confidentiality and privacy of the collected information. The design and development of the myoelectric prosthesis prototype were carried out ethically, without direct tests on children, focusing exclusively on collecting and analyzing anthropometric data to ensure the safety and well-being of the participants involved in the study.

### *Instruments*

The mechanical parts of the prosthesis were manufactured using additive digital manufacturing methods, specifically 3D printing, using detailed FDM and SLA techniques. 3D printing was performed using the Creality Ender-5 Plus printer, an extended version of the Ender series with a print format of 350x350x400 mm. The printing precision is approximately 0.1 mm, and the extruder can reach up to 260°C, with a speed of up to 80 mm/s. To evaluate and verify circuits related to the acquisition, amplification, and filtering of bio-potentials, a Tektronix oscilloscope, specifically the TBS 2000B model, was used.

Finally, Autodesk Fusion 360 (2019) software was used for prototype design and finite element analysis.

## *Mechanical Design*

*Prototype design / CAD*

Fusion 360 was employed to design and functionally analyze the prosthesis, using the right upper limb as a reference. Force and pressure tests were conducted through finite element analysis in the software, enabling design adjustments without the need for physical prototypes. The outcome is a stable and functional prototype.

*Finger, palm, and socket design*

Fusion 360 was employed to design and functionally analyze the prosthesis, using the right upper limb as a reference. Force and pressure tests were conducted through finite element analysis in the software, enabling design adjustments without the need for physical prototypes. The outcome is a stable and functional prototype.

*Table 1. Dimensions of the phalanges of the fingers.*

| Finger | Proximal | Medial | Distal |
|---|---|---|---|
| Pulgar | 29.3 cm | | 20.48 cm |
| Indicé | 32.65 cm | 15.07 cm | 15.3 cm |
| Medio | 29.77 cm | 23.63 cm | 11.71 cm |
| Anular | 25.95 cm | 17.49 cm | 16.44 cm |
| Meñique | 22.62 cm | 15.03 cm | 13.2 cm |

A mechanism based on tendons will be adopted to facilitate flexion and extension movements. A cable, when tensioned, will induce joint flexion, as illustrated in Figure 1. This principle governs the extension mechanism, requiring channels in all phalanges to guide the cables acting as tendons.

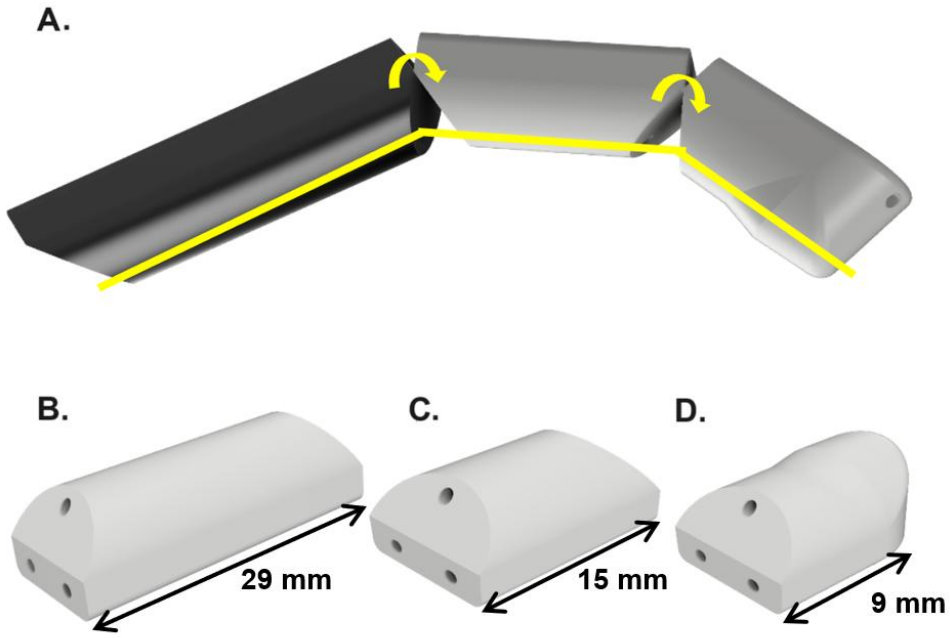


Figure 1. (A). the yellow arrows identify CAD design of the phalanges and the rotation direction, and yellow lines indicate the direction of flexion tendons. CAD design of the phalanges (B) Proximal, (C) Medial, and (D) Distal.

The modeling of the palm was based on a calibrated image of the volunteer's hand integrated into the CAD software. Anthropometric measurements are derived from the average palm length and hand width. The design includes channels for the tendon and a securing hole. A tendon mechanism for flexion and extension will be implemented using cables guided by channels in all phalanges.

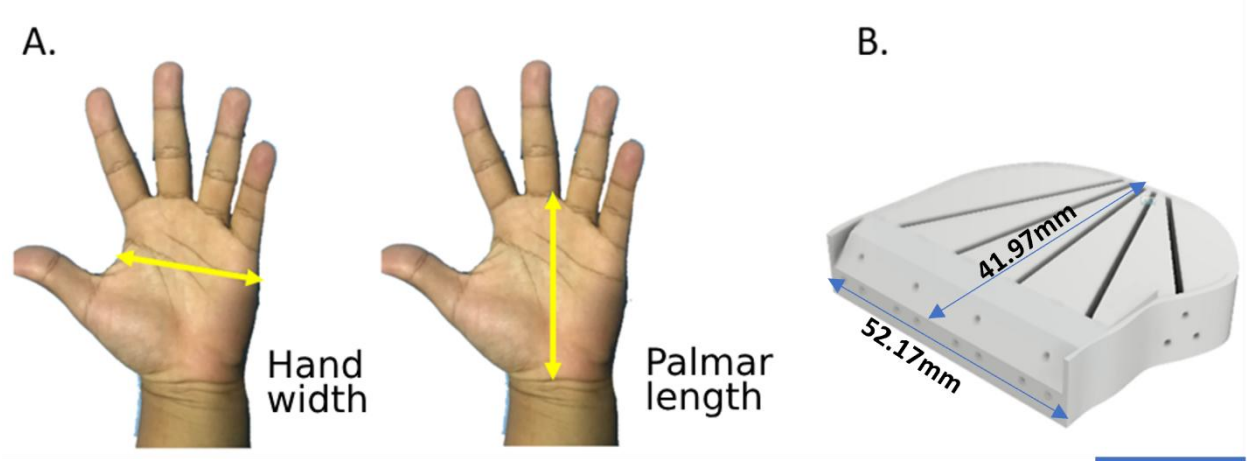


Figure 2. A. Anthropometric measurements used for the design; B. palm design. The scale bar represents 20 mm.

The socket design was based on anthropometric measurements of the forearm's distal, medial, and proximal portions. The image capture method of the volunteer's forearm was calibrated with the average anthropometric measurement corresponding to the complete forearm length and divided into three portions. Finally, extrusion and modifications to the piece were carried out to create the parts for attachment to the stump and interconnection with the palm piece.

### *Electromyography System Design*

In the EMG signal acquisition system, depicted in Figure 3, there is a distinct stage for signal acquisition and pre-amplification, followed by a filtering stage. For the envisioned device, a second amplification or conditioning stage is added to adjust signal voltage values, enabling processing by a microcontroller. The amplitude of the target biopotential is within the range of 10 mV. Subsequently, an actuation stage is integrated, responsible for executing movements in response to the signal captured by the implemented EMG system.

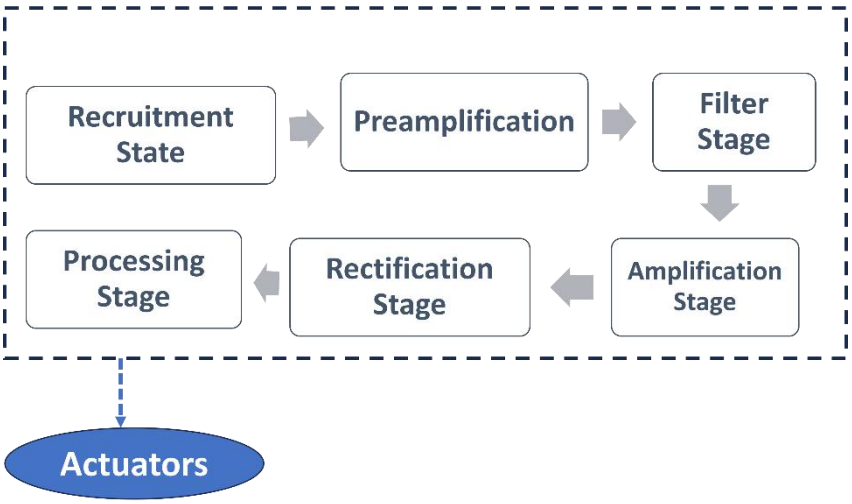


Figure 3 Block diagram of the acquisition and processing system.

### *Signal acquisition*

SENIAM recommendations were followed to capture surface electromyography signals using pre-gelled silver/silver chloride surface electrodes. These disposable Kendall MEDITRACE electrodes, with conductive gel, were chosen for their easy handling and improved conductivity and impedance conditions. A bipolar configuration was adopted by placing two electrodes in parallel to the direction of the muscle fiber, along with a third reference electrode in an electrically unaffected area.

### *Pre-amplification and Filtering*

As for the pre-amplification of the EMG signal, an instrumentation amplification module was implemented. Its design is based on the AD620 reference differential amplifier, chosen for its common-mode rejection characteristics, low offset voltage, and cost-effectiveness.

The EMG card's filtering stage consists of a bandpass filter comprising a high-pass filter and a low-pass filter, with cutoff frequencies set at 50 Hz for the high-pass filter and 500 Hz for the low-pass filter. Typically, the high-pass filter is established between 10 and 20 Hz. The lower frequencies in the signal spectrum correspond to motor muscle firing mechanisms and do not significantly contribute to the gesture recognition system. Additionally, a Notch filter is introduced with a cutoff frequency of 60 Hz to reduce noise caused by the power grid. The Notch filter is designed to eliminate a specific frequency component with its selective response. In other words, this filter only applies attenuations to the specified frequency, in our case, the 60 Hz from the power source.

A Twin T Notch filter is implemented with the following transfer function (Electrical and Computer Engineering Support and Tech, 2012) (Seijas, 2013):

$$H_{(S)} = \frac{\alpha(s^2+{\omega_0}^2)}{s^2+4(1-\alpha)\omega_0 * s+{\omega_0}^2} \qquad (1)$$

where $\omega_0$ : Notch filter cutoff frequency; $\alpha$: feedback factor (gain) $\delta$: damping Factor. Rewriting Equation (1) in terms of the components, we have:

$$H_{(S)} = \frac{\alpha(R^2C^2s^2+1)}{R^2C^2s^2+2(2-\alpha)*RCs+1} \qquad (2)$$

Fort he filter $\omega_0 = 2\pi f_c = 2\pi * 60Hz = 376.99\ {}^{rad}/_{S}$

For an α = 1, the damping δ is 0, indicating an underdamped response. The theoretically infinite Q factor represents a high-Q Notch Twin T filter. In Figure 4, the implemented Notch filter is visualized and designed without resistors or feedback amplifiers to control the α Factor. The removal of the feedback network, similar to a voltage follower, results in the maximum possible Q of the filter, as illustrated in Figure 5, showing the frequency response of the implemented filter.

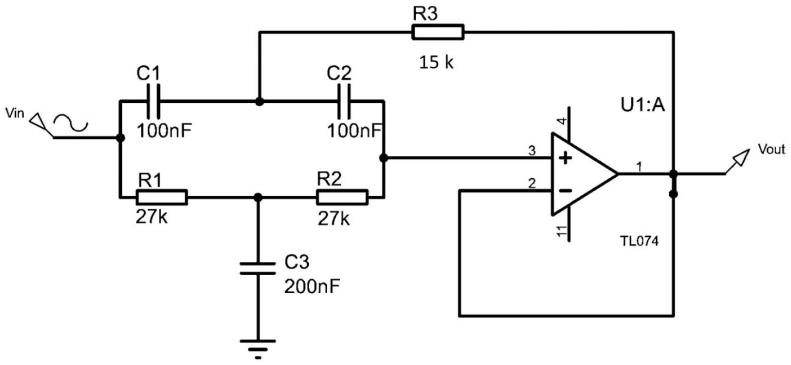


Figura 4. Notch Filter

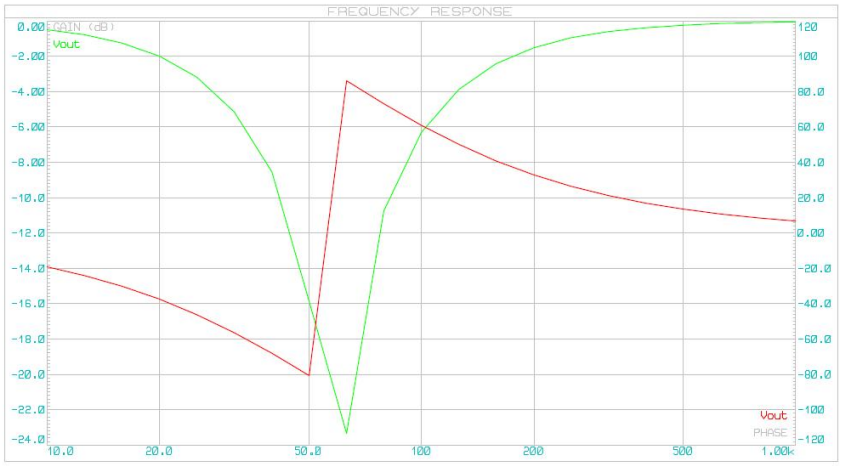


Figure 5. In green is the frequency response, and in red is the phase of the implemented Notch Filter using 5% tolerance carbon resistors with a high-temperature coefficient of 1500 ppm/ºC.

### *Bandpass Filter, Amplification, Rectification, and Signal Conditioning*

A third-order bandpass filter was also designed, consisting of two series-connected filters: a low-pass filter with a cutoff frequency of 500 Hz and a high-pass filter with a cutoff frequency of 60 Hz. For the high-pass filter, an operational amplifier was configured in non-inverting mode with an adjustable gain (A) ranging from 50 to 150. Subsequently, a rectification stage was implemented for the output signal to be correctly read by the microcontroller. A precision full-wave rectifier circuit, capable of transmitting one polarity of the input signal and inverting the other, was employed for this purpose(Coughlin & Driscoll, 2000).

To adapt the signal obtained in the previous stages, the Arduino Nano was used as a component to shape the EMG system signal, activating the actuators. The Arduino reads the voltage signal obtained by the capture system, emitted by the EMG board in voltage ranges from 0 to 5V. However, the Arduino reads this signal from 0 to 1023 bits. After obtaining this information, the Arduino filters and compares the values to activate the actuators accordingly, rotating in one direction, the other, or stopping, based on the specified limits. The input voltage range for this element varies from 5V to 12V. The Arduino internally incorporates a DC/DC converter to function normally and provide voltages of 3.3 and 5 volts

### *Tests*

To verify the functionality of the acquisition system, capturing tests were conducted in which 5 participants were asked to hold an object and maintain the applied force for 3 seconds. The objective was to observe the variation in the EMG signal under constant contraction, recorded with the developed system, and compare these results with commercial sensors.

In the second trial, the proof of concept was executed to confirm the system's operation. This involved integrating the acquisition circuit with the prosthesis's mechanical parts, ensuring that the phalanges' flexion and extension were achieved in response to the captured biopotential.

## 3. Results

### *Anthropometric measurements.*

The data collection results are observed in the following tables on the anthropometry of the upper limb; these data were obtained through a survey, and the sample was conveniently chosen with a total of seven participants aged 2-3 years, including 3 males and 4 females. In Table 1, the variability observed in anthropometric measurements reflects the inherent diversity in the population of children aged 2 to 3 years. It is essential to consider these differences when designing specific devices for this age group, such as the myoelectric prosthetic prototype. The inclusion of

standard deviations highlights the dispersion of the data. It can guide the precision required to manufacture the device to adapt to the individual dimensions of potential users.

Table1: Summary of Anthropometric Measurements in 2-3-Year-Old Children.

| Medida/Dimensión | Femenino | Masculino | Total |
|---|---|---|---|
| Estatura | 91.75 ± 7.62 cm | 99.1 ± 4.36 cm | 95.43 ± 6.41 cm |
| Long. Miembro Sup. | 39.41 ± 1.93 cm | 42.5 ± 1.89 cm | 41.96 ± 1.91 cm |
| Long. Antebrazo | 15.18 ± 2.81 cm | 17.5 ± 7.58 cm | 16.34 ± 5.02 cm |
| Diám. de Agarre | 29.71 ± 7.34 mm | 34.75 ± 5.01 mm | 32.23 ± 6.19 mm |
| Falange Distal 1 | 20.04 ± 3.07 mm | 23.24 ± 1.82 mm | 21.64 ± 3.47 mm |
| Falange Distal 2 | 23.02 ± 2.38 mm | 16.46 ± 4.29 mm | 19.74 ± 5.67 mm |
| Falange Distal 3 | 22.83 ± 3.76 mm | 17.92 ± 3.12 mm | 20.28 ± 4.41 mm |
| Falange Distal 4 | 17.6 ± 1.14 mm | 18.15 ± 0.43 mm | 17.88 ± 1.74 mm |
| Falange Distal 5 | 20.71 ± 1.84 mm | 16.35 ± 1.68 mm | 18.53 ± 2.1 mm |
| Falange Medial 2 | 20.04 ± 1.59 mm | 24.51 ± 3.06 mm | 22.83 ± 3.29 mm |
| Falange Medial 3 | 23.02 ± 3.76 mm | 24.5 ± 1.09 mm | 23.39 ± 2.03 mm |
| Falange Medial 4 | 22.83 ± 1.86 mm | 18.15 ± 0.46 mm | 20.49 ± 2.75 mm |
| Falange Medial 5 | 17.6 ± 2.72 mm | 20.71 ± 1.79 mm | 19.16 ± 2.2 mm |
| Falange Prox. 1 | 20.04 ± 4.15 mm | 23.02 ± 4.37 mm | 21.54 ± 3.82 mm |
| Falange Prox. 2 | 23.02 ± 4.19 mm | 22.83 ± 3.74 mm | 22.93 ± 3.96 mm |
| Falange Prox. 3 | 22.83 ± 4.27 mm | 17.6 ± 1.97 mm | 20.22 ± 4.23 mm |
| Falange Prox. 4 | 17.6 ± 2.26 mm | 20.71 ± 4.24 mm | 19.16 ± 2.64 mm |
| Falange Prox. 5 | 25.43 ± 4.69 mm | 26.35 ± 3.76 mm | 25.34 ± 4.1 mm |
| Long. Palmar Vert. | 56.7 ± 4.3 mm | 61.02 ± 2.77 mm | 58.89 ± 3.89 mm |
| Long. Palmar Hor. | 45.97 ± 4.14 mm | 49.11 ± 2.64 mm | 47.54 ± 3.49 mm |

## *FEA*

Boundary conditions were applied, restricting movement in the socket piece while allowing sliding in the distal phalanges of the fingers. For this study, the cylindrical grip position of an object with an approximate diameter of 30 mm was considered, and two cases were evaluated. The selected material for all prototype parts was polylactic acid (PLA) filament, with an elastic modulus of 3.98 GPa. Other necessary mechanical properties for creating the material are detailed in Table 16 and were obtained from sources (Pinto, y otros, 2015) and (Anderson, 2017) ; the PLA used has a Young's modulus of 3.98 GPa and a Poisson's ratio of 0.332.

In the first test, the prototype sustained a 2 N load, resulting in a maximum stress of 64.12 MPa under the cylindrical grip condition. This stress is concentrated at the junction between the palm and the proximal part of the first phalanx, corresponding to the thumb of the prototype. The critical safety factor in the mentioned area is 0.016, ensuring proper functioning. Additionally, a maximum displacement of 0.45 mm at the most distal part of the thumb is recorded, as shown in Figure 5 (Panel A), but this result is not considered significant. In the second test, the same grip type was maintained but with the object resting on the palm, as illustrated in Figure 5. In this configuration, the safety factor reaches a minimum of 0.015.

On the other hand, when analyzing the stress distribution, a maximum of 65.29 MPa is identified in the most distal region of the thumb, as shown in Figure 5 (Panel B). Regarding displacement, a maximum value of 0.46 mm at the most distal part of the thumb is recorded, as visualized in the figure. It is worth noting that this result is not considered significant.

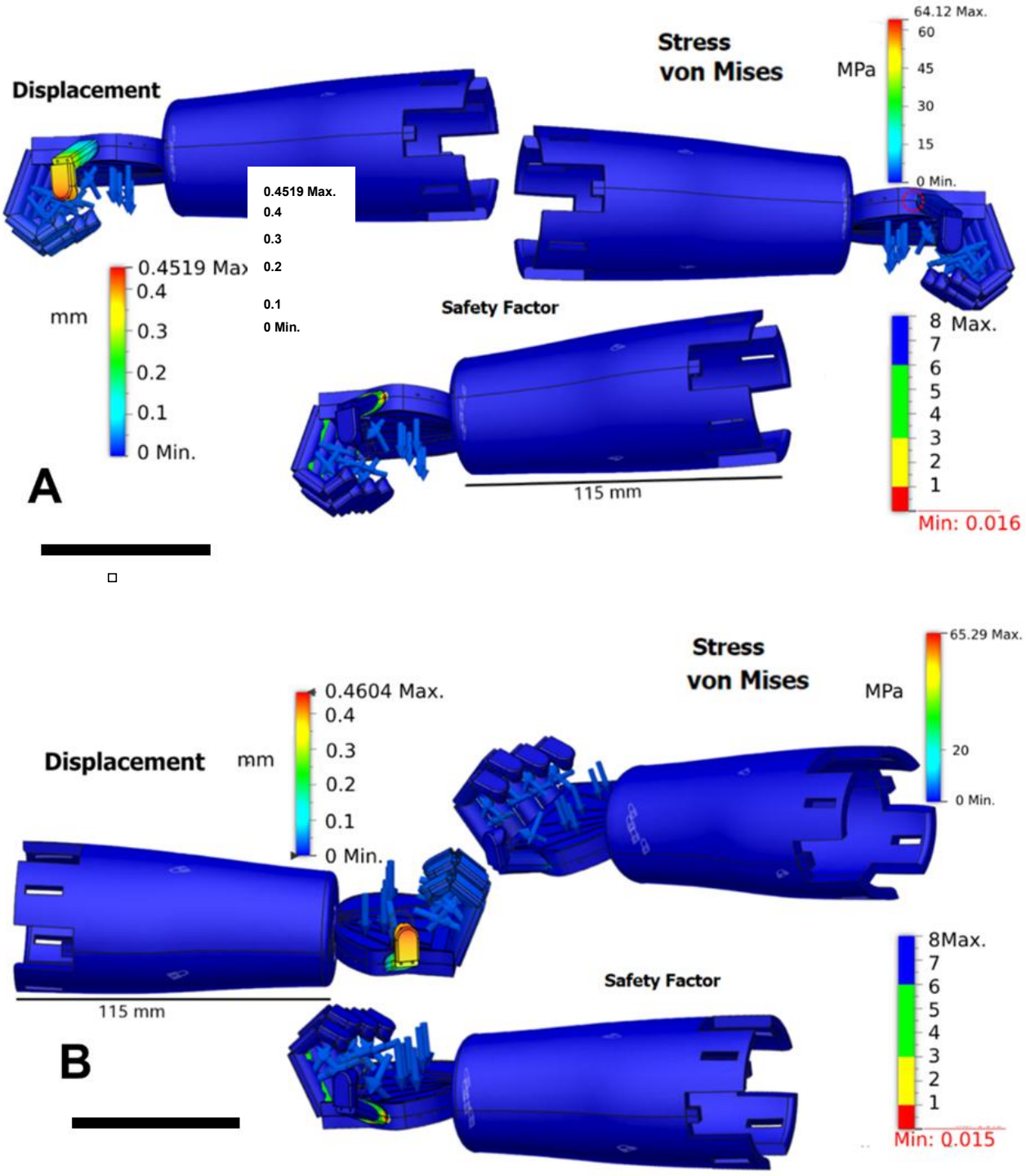


Figure 6: **Panel A**. Cylindrical grip with a 2N load. **Panel B**. 2N load resting on the palm in a cylindrical grip. The scale bar represents 20 mm.

### *Electromyographic Signal Acquisition*

In this test, participants are asked to hold an object and maintain the applied force for 3 seconds. The purpose is to observe the variation in the EMG signal under constant contraction and determine the repeatability of the acquisition.

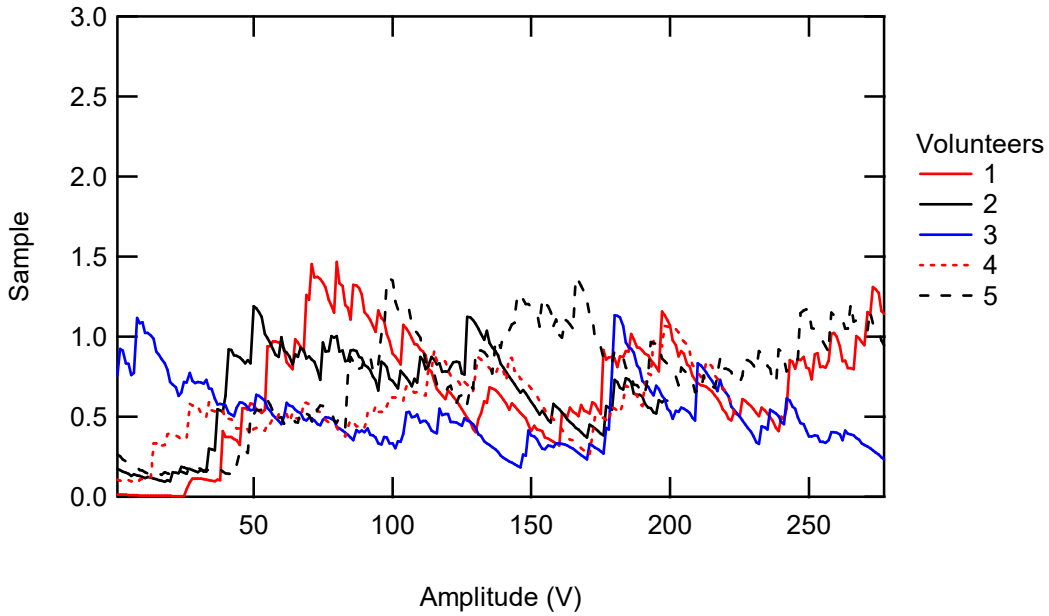


Figure 6. Comparison of the maximum and minimum ranges of the EMG amplitude of the joint superficial flexor muscle of the fingers.

In Figure 6, a comparison of the amplitude of the electromyography signal of the joint superficial flexor muscle of the fingers during sustained flexion is observed. The average of this signal was compared with the results obtained by (Bermeo Varon, y otros, 2019), who, using the MyoWare™ Muscle Sensor (AT-04-001), received minimum amplitude ranges of 0.775 V and a maximum of 0.868 V.

The data underwent a one-way ANOVA test, yielding a p-value of 0.252, higher than the significance level of 0.05. This indicates no significant difference in the average voltage among the different data points collected from the participants. The results are summarized in Table 3. A means comparison was conducted to assess the similarity in the data captured by the prototype. As observed, none of the p-values is less than the significance level of 0.05. This means we cannot reject the null hypothesis for any data points. Therefore, we can conclude that there is no significant difference in the average voltage among data points.

Table 2: ANOVA statistical tests and comparison of means.

| ANOVA | | | | | |
|---|---|---|---|---|---|
| Source of Variation | SS | df | Mean square | F-Value | P value |
| Between Groups | 2.5 | 4 | 0.63 | 1.57 | **0.252** |
| Within Groups | 10 | 5 | 2 | | |
| Total | 12.5 | 9 | | | |

| Means Comparison | | | | | |
|---|---|---|---|---|---|
| Data Point | Mean Voltage | Standard Deviation | t-value | p-value | Data Point |
| P02 | 5.2V | 0.5V | 1.04 | 0.328 | P02 |
| P03 | 5.4V | 0.6V | 1.2 | 0.262 | P03 |
| P04 | 5.6V | 0.7V | 1.36 | 0.217 | P04 |
| P05 | 5.8V | 0.8V | 1.52 | 0.164 | P05 |
| P06 | 6.0V | 0.9V | 1.68 | 0.131 | P06 |

Trial 2 follows a similar sequence to Trial 1, applying the designed prototype's activation to assess the prototype's reaction time, not the acquisition system. For this, the volunteer will be asked to perform five hand closures and openings within a specified time.

Upon concluding Trial 2, the proof of concept for the prototype was verified. Upon analyzing the video obtained (access ZENODO link) for this trial, the correct functionality of the proposed prototype in terms of finger flexion and extension was confirmed.

## 4. Conclusion

Most of the designed prostheses are focused on adults. The few options developed for pediatric purposes are intended for children who have been amputated due to accidents or illnesses. However, there are no suitable designs for patients with transverse agenesis (congenital amputation). Additionally, prosthetics are not affordable for Panamanian families due to their economic reality.
This paper presents the progress in designing and constructing a prototype of a right-hand myoelectric prosthesis. The design is based on the average anthropometric measurements of 7 infants aged 2-3 years, with an average height of around 91 cm.
Finite element analysis tests were conducted on the prototype structures to determine areas of concentration of higher stress, with the highest stress being 64.12 MPa located at the junction between the palm and the proximal phalanx of the thumb.
A system for capturing electromyographic signals is presented, with the average value ranges falling within the parameters obtained by commercially available EMG sensors, ranging from 0.775 V to 0.868 V. After processing, these signals can be applied to the prototype's actuation system.

## Referencias

Anderson, I. (2017). Mechanical Properties of Specimens 3D Printed with Virgin and Recycled Polylactic Acid. *3D Printing and Additive Manufacturing*, 110-115. Retrieved from https://doi.org/10.1089/3dp.2016.0054

Ayuso, S. (2018). Bebés nacidos sin un brazo o una mano, el misterio que inquieta a Francia. *EL PAIS*.

Banco Mundial. (2021). El apoyo del Banco Mundial ante la COVID-19 en ALC. Retrieved from https://www.bancomundial.org/es/country/panama/overview

Bastarrechea, A., Estrada, Q., Zubrzycki, J., Torres-Argüelles, V., & Reynoso, E. (2020). Mechanica design of a low cost-cost ABS hand prosthesis using the finite element method. *Journal of Physics: Conference Series, 19*(16), 1-11.

Bermeo Varon, L., Bravo, A., Perez, V., Arcos, E., Quiguanas, D., & Villarejo, J. (2019). Protocolo para la adquisicion de senales mioelectricas de los musculos inervados por los nervios ulnar, medial y radial para ortesis de mano. 49.

Bethge, M., Von Groote, P., Giustini, A., & Gutenbrunner, C. (2014). The world report on disability: A challenge for rehabilitation medicine. *American Journal of Physical Medicine and Rehabilitation*, 93. Retrieved from https://doi.org/10.1097/PHM.0000000000000016

Budinski, S., Manojlović, V., & Knežević, A. (2021). Predictive Factors for Succesful Prosthetic Rehabilitation After Vascular Transtibial Amputation. *Acta Clinica Croatica, 60*(4), 657-664.

Burn, M. B., & Gogola, G. R. (2016). Three-dimensional printing of prosthetic hands for children. *Journal of Hand Surgery*, 103-109. Retrieved from https://doi.org/10.1016/j.jhsa.2016.02.008

Cabrera, M. (2012). Dos hospitales catalanes revolucionan la ortopedia.

Coughlin, R. F., & Driscoll, F. F. (2000). *Operational Amplifiers & Linear Integrated Circuits.*

Davids, J. R., Wagner, L. V., & Meyer, L. C. (2005). Prosthetic management of children with unilateral congenital below-elbow deficiency. *Journal of Bone and Joint Surgery - Series A*, 12994-1300. doi:10.2106/JBJS.E.00982

Dy, C. J., Swarup, I., & Daluiski, A. (2014). Embryology, diagnosis, and evaluation of congenital hand anomalies. *Current Reviews in Musculoskeletal Medicine*, 60–67.

Electrical and Computer Engineering Support and Tech, I. V. (2012). Twin. T. Notch Filter. Retrieved from https://filebox.ece.vt.edu/~LiaB/ECE3074/Lectures/%0APowerpoint/Twin_T_Notch.pdf

Enable Community Foundation. (2017). Comunity focused on using of 3D printing technology used in upper limb prosthesis. Enable Community Foundation.

FAULHABER. (2017). Bebionic myoelectric hand prosthesis. *Today's Medical Developments.*

Fleming, A., Huang, S., Buxton, E., Hodges, F., & Huang, a. H. (2021). Direct continuous electromyographic control of a powered prosthetic ankle for improved postural control after guided physical training: A case study. *Wearable Technology, 2*(e3), 1-26.

Gishen, K., & Askari, M. (2014). Congenital hand anomalies: Etiology, classification, and treatment. *Journal of Craniofacial Surgery*, 284–294.

Hermansson, L. (2004). Upper Limb Reduction Deficiencies.

Huizing, K., Reinders-Messelink, H., Maathuis, C., Hadders-Algra, M., & Sluis, C. (2010). Age at first prosthetic fitting and later functional outcome in children and young adults with unilateral congenital below-elbow deficiency: A cross-sectional study. *Prosthetics and Orthotics International, 34*(2), 166-174.

IMPACTO POSITIVO. (2020). Primera prótesis biónica es creada en Panamá. Retrieved from https://somosimpactopositivo.com/gente-que-inspira/protesis-bionica/

James, M. A., Bagley, A. M., Brasington, K., Lutz, C., McConnell, S., & Molitor, F. (2006). Impact of prostheses on function and quality of life for children with unilateral congenital below-the-elbow deficiency. *Journal of Bone and Joint Surgery - Series A*, 2356–2365. doi:10.2106/JBJS.E.01146

Kate, J. T., Smit, G., & Breedveld, P. (2017). 3D-printed upper limb prostheses: a review. *Disability Rehabil Assist Technol, 12*(3), 300-314.

Koprnicky, J. N. (2017). 3D printed bionic prosthetic hands. *Koprnicky, J., Najman, P., & Safka, J.* Retrieved from https://doi.org/10.1109/ECMSM.2017.7945898

Limbitless Solutions. (2016). Creating Hope With 3d Printed Limbs. Retrieved from http://www.limbitless-solutions.org/

MEDIPRAX. (2020). *Prótesis para niños con agenecia de mano.* Retrieved from https://aparatosortopedicos.com/protesis-para-ninos-con-agenecia-de-mano/

My Human Kit. (2017). DIY and Digital Fabrication for humans, both disabled or not. Retrieved from http://myhumankit.org/en/home-2/

Not Impossible. (2016). Not Impossible. Retrieved from http://www.notimpossible.com/

Open Bionics. (2017). Open Bionics. Retrieved from https://www.openbionics.com/

Össur. (2018). i-Limb® Ultra. Retrieved from https://www.ossur.com/en-us/prosthetics/arms/i-limb-ultra

Ottobock. (2017). Michelangelo prosthetic hand. Retrieved from https://www.ottobockus.com/prosthetics/upper-limb-prosthetics/solution-overview/michelangelo-prosthetic-hand/

Peerdeman, B., Boere, D., Witteveen, H., Huis, R., & Hermie Hermens, S. S. (2017). Myoelectric prostheses: State of the art from a user-centered perspective. *Journal of Rehabilitation Medicine, 49*(7), 559-568.

Pinto, V. C., Ramos, T., Alves, S., Xavier, J., Tavares, P., Moreira, P. M., & Guedes, R. M. (2015). Comparative Failure Analysis of PLA, PLA/GNP and PLA/CNT-COOH Biodegradable Nanocomposites thin Films. *Procedia Engineering*(114), 635–642. Retrieved from https://doi.org/10.1016/j.proeng.2015.08.004

Range of Motion Project. (2015). Range of Motion Project. Retrieved from http://www.rompglobal.org/

Resnik, L., Meucci, M. R., Lieberman-Klinger, S., Fantini, C., Kelty, D. L., Disla, R., & Sasson, N. (2012). Advanced upper limb prosthetic devices: Implications for upper limb prosthetic

rehabilitation. *Archives of Physical Medicine and Rehabilitation*, 710-717. Retrieved from https://doi.org/10.1016/j.apmr.2011.11.010

Rodríguez, J. A. (2010). Situación de las personas con discapacidad en Panamá.

Sato, Y., Kaji, M., & Oizumi, T. T. (1999). Carpal tunnel syndrome involving unaffected limbs of stroke patients. *Stroke, 30*(2), 414-418.

Seijas, C. (2013). *Apuntes de Electrónica III.*

Sociedad Española de Cirugía Ortopédica y Traumatología. (2010). *Manual de Cirugía Ortopédica y Traumatología*.

Sorbye, R. (1980). Myoelectric prosthetic fitting in young children. *Clinical Orthopaedics Rel. Res, 148*, 34-40.

Vasluian, E., de Jong, I. G., Janssen, W. G., Poelma, M. J., Van Wijk, I., & Reinders-Messelink, H. A. (2013). Opinions of Youngsters with Congenital Below-Elbow Deficiency, and Those of Their Parents and Professionals Concerning Prosthetic Use and Rehabilitation Treatment. *PLOS ONE*. doi:10.1371

Youbionic. (2017). Youbionic. Retrieved from http://www.youbionic.com/

Zarante, I., Franco, L., López, C., & Fernández, N. (2010). Frequencies of congenital malformations: assessment and prognosis of 52,744 births in three cities of Colombia. *Biomedica*, 65--71. Retrieved from https://doi.org/10.7705/biomedica.v30i1.154

## Conflict of Interest

The authors declare that there are no conflicts of interest.